Single-layer Decoupling Networks for Circulant Symmetric Arrays

Jacob C. Coetzee, James D. Cordwell, Elizabeth Underwood and Shauna L. Waite

School of Engineering Systems, Queensland University of Technology, GPO Box 2434, Brisbane QLD 4001, Australia

Abstract

Reduced element spacing in antenna arrays gives rise to strong mutual coupling between array elements and may cause significant performance degradation. These effects can be alleviated by introducing a decoupling network consisting of interconnected reactive elements. The existing design approach for the synthesis of a decoupling network for circulant symmetric arrays allows calculation of element values using closed-form expressions, but the resulting circuit configuration requires multilayer technology for implementation. In this paper, a new structure for the decoupling of circulant symmetric arrays of more than four elements is presented. Element values are no longer obtained in closed form, but the resulting circuit is much simpler and can be implemented on a single layer.

Keywords
Adaptive arrays, Antenna array feeds, Antenna arrays, Decoupling networks, Mutual coupling.

1. Introduction

In wireless systems, spatial diversity can achieve significant gain in system capacity [1]. The effects of mutual coupling in arrays are usually restricted by using an inter-element spacing of at least half a wavelength ($\lambda/2$). However, for antenna diversity in mobile applications, the use of an element spacing considerably smaller than $\lambda/2$ becomes inevitable. Reduced element spacing results in increased coupling between array elements, which will decrease the antenna gain considerably and thus cause significant system performance degradation [2,3].

The effects of mutual coupling can be countered by using passive, lossless decoupling and matching networks. A decoupling network consists of interconnected reactive elements and/or transmission line sections and stubs. It provides an additional signal path between the array elements, which effectively cancels the external coupling between them. The decoupling network for an N-port array is a $2N$-port network with N ports connected to the array elements, while the remaining N ports represent the isolated input ports. Various implementations of decoupling networks (DN) have been described in the literature [4-9], but investigations have largely been limited to a small number of radiators.

For maximum versatility, the number of elements in an adaptive array needs to be as large as possible. Recently, a systematic design approach for larger circulant symmetric arrays was proposed [10]. The design procedure involves the repeated decoupling of the characteristic eigenmodes of the array. The method is uncomplicated and allows calculation of element values using closed-form expressions, but the resulting circuit configuration is complex. For example, the decoupling network for an array of $N>5$ elements would require a circuit with at least three different layers.

In this paper, we propose a new structure for the decoupling of circulant symmetric arrays of $N>5$ elements. Network element values are still obtained through a process of repeated eigenmode decoupling, but in this case by solving sets of nonlinear equations. Although the design procedure is more complicated, the resulting decoupling network can be implemented on a single layer.

2. Theory

Consider a circulant symmetric array comprising N elements equally spaced on the circumference of a circle. The port voltages and port currents of the array are thus related by

$$\mathbf{V} = \mathbf{Z^a} \, \mathbf{I}, \tag{1}$$

where $\mathbf{V}=[V_1, V_2, ..., V_N]^T$ and $\mathbf{I}=[I_1, I_2, ..., I_N]^T$ are the voltage and current vectors, respectively, and $\mathbf{Z^a}$ is the symmetric impedance matrix of the array. $\mathbf{Z^a}$ will have N eigenvalues and N corresponding orthogonal eigenvectors. Eigenmode m is excited when the port currents are proportional to eigenvector $\mathbf{e}_m$. The eigenvectors form a complete basis for the port currents so that any conceivable excitation can be expressed as

$$\mathbf{I} = \sum_m c_m \mathbf{e}_m, \qquad (2)$$

with c_m being the excitation coefficient of mode m. Using Equation 1, the port voltages are obtained as

$$\mathbf{V} = \mathbf{Z}^a \left(\sum_m c_m \mathbf{e}_m \right) = \sum_m c_m Z_m \mathbf{e}_m, \qquad (3)$$

where Z_m is the eigenvalue corresponding to eigenvector $\mathbf{e}_m$. The input impedance at port i is given by

$$Z_i^{\mathrm{in}} = \frac{V_i}{I_i} = \frac{\sum_m c_m Z_m e_{mi}}{\sum_m c_m e_{mi}}, \qquad (4)$$

where e_{mi} is the ith element of $\mathbf{e}_m$. From Equation 4, it is clear that the input impedance is dependent on the port excitations, which is a well-known consequence of mutual coupling between the array elements. When a single mode is excited, the input impedance reduces to $Z_i^{\mathrm{in}} = Z_m$. The eigenvalue Z_m therefore represents the input impedance observed at each port when the port currents or voltages are proportional to eigenvector $\mathbf{e}_m$.

Decoupling of an array involves a process of modifying its impedance matrix to reduce all the off-diagonal elements to zero. An alternative approach involves a process of matching the modal input impedances. Suppose the impedance matrix of the array is modified by connecting additional circuitry to the array ports to yield a new impedance matrix $\mathbf{Z}'$. If $\mathbf{Z}'$ has the same eigenvectors as before, but all the modal impedances are equal (i.e. $Z_m = Z_0'$), Equation 3 reduces to

$$\mathbf{V} = Z_0' \sum_m c_m \mathbf{e}_m. \qquad (5)$$

From Equation 4, the input impedance at each port becomes $Z_i^{\mathrm{in}} = Z_0'$, which is independent of the port excitations. For circulant symmetric arrays, array decoupling can therefore also be accomplished by equalizing the eigenvalues of the impedance matrix of the array.

An N-element array characterized by a circulant impedance matrix with k distinct eigenvalues requires a decoupling network with $2(k-1)$ independent parameters. In [10], it was shown that array decoupling can be accomplished in $(k-1)$ stages by using a ladder of circulant symmetric network configurations (stage networks). Each stage network consists of N identical series reactive elements and N identical parallel reactive elements. The parallel elements can be arranged in the

shape of a single polygon, several smaller polygons rotated with respect to one another or in the shape of a star with or without a common node at the center. In order to decouple the array, $(k-1)$ suitable stage networks have to be identified. Two modes with distinct eigenmode impedances are decoupled during each stage by calculating the elements of the stage network using closed-form expressions. The order in which the stage networks are employed is critical to ensure that the equality of the eigenmode impedances is preserved in subsequent states. Since all element values are calculated in closed form, the synthesis procedure is very simple. However, the complexity of the composite network complicates its implementation.

In this paper, we present an alternative geometry for the decoupling circuit. For an N-element array characterized by a circulant impedance matrix with k distinct eigenvalues, all the first $(k-2)$ stage networks consist of N series reactive elements and N parallel reactive elements arranged in the shape of a single polygon. This ladder of stage networks is employed to decouple $(k-1)$ eigenmodes, which involves the numerical solution of a set of $2(k-2)$ nonlinear equations to determine the $2(k-2)$ reactive elements. The final stage network consists of N series reactive elements and N parallel reactive elements arranged in the shape of an N-legged star with a common node in the center. This stage network is used to decouple the lowest-order eigenmode and the other modes. The two reactive components of the final stage network can be determined using the closed-form relations provided in [10]. The composite decoupling network yields uncoupled ports for the array. The uncoupled port impedances can be matched to the system impedance Z_0 using suitable matching networks. For each reactive element in the decoupling and matching network, the value of a corresponding inductor or capacitor may be computed at the center frequency. The decoupled array can thus be analyzed as a function of frequency. The application of this approach is best illustrated by considering the following two examples.

2.1 Design Example: 6-Element Array

The method presented in [10] was illustrated by considering a 6-element circulant symmetric array. The impedance matrix of such an array is given by

$$\mathbf{Z}^a = \begin{bmatrix} Z_{11}^a & Z_{12}^a & Z_{13}^a & Z_{14}^a & Z_{13}^a & Z_{12}^a \\ Z_{12}^a & Z_{11}^a & Z_{12}^a & Z_{13}^a & Z_{14}^a & Z_{13}^a \\ Z_{13}^a & Z_{12}^a & Z_{11}^a & Z_{12}^a & Z_{13}^a & Z_{14}^a \\ Z_{14}^a & Z_{13}^a & Z_{12}^a & Z_{11}^a & Z_{12}^a & Z_{13}^a \\ Z_{13}^a & Z_{14}^a & Z_{13}^a & Z_{12}^a & Z_{11}^a & Z_{12}^a \\ Z_{12}^a & Z_{13}^a & Z_{14}^a & Z_{13}^a & Z_{12}^a & Z_{11}^a \end{bmatrix}. \qquad (6)$$

The eigenvalues of the impedance matrix are
$Z_a = Z_{11}^a + 2Z_{12}^a + 2Z_{13}^a + Z_{14}^a$,
$Z_b = Z_{11}^a - 2Z_{12}^a + 2Z_{13}^a - Z_{14}^a$,
$Z_c = Z_d = Z_{11}^a - Z_{12}^a - Z_{13}^a + Z_{14}^a$
and $Z_e = Z_f = Z_{11}^a + Z_{12}^a - Z_{13}^a - Z_{14}^a$, while the corresponding orthogonal eigenvectors are $\mathbf{e}_a = [1, 1, 1, 1, 1, 1]^T$, $\mathbf{e}_b = [1, -1, 1, -1, 1, -1]^T$, $\mathbf{e}_c = [1, 0, -1, 1, 1, 0, -1]^T$, $\mathbf{e}_d = [1, -1, 0, 1, -1, 0]^T$, $\mathbf{e}_e = [1, 0, -1, -1, 0, 1]^T$ and $\mathbf{e}_f = [1, 1, 0, -1, -1, 0]^T$. Since there are four distinct eigenvalues, three stage networks are required to decouple the eigenmodes. The stage networks are shown in the second column of Table 1. A stage network will reduce to the equivalent circuit shown in Figure 1 for each eigenmode. The parameter n_{im} in Figure 1 for stage network type i can be determined by assuming port voltages corresponding to eigenvector m and using

circuit analysis to obtain the equivalent network. As an example, the derivation of the equivalent circuit for stage network 1 and eigenmode c is shown in Figure 2. In Figure 2(a), port voltages corresponding to $\mathbf{e}_c$ are applied to the new external ports, while the original ports are terminated in the array input impedance for mode c, Z_c. The undriven ports are grounded and an electrical conductor is introduced on the symmetry plane in Figure 2(b). The resulting equivalent circuit is shown in Figure 2(c), and comparing this result to Figure 1 yields $n_{1c} = 3$. Equivalent circuits for the other stage networks and eigenmodes can be determined in a similar way. The parameter n_{im} for stage network type i and eigenmode m is shown in the third column of Table 1. A composite decoupling network is obtained by cascading the three stage networks, as depicted in Figure 3. The equivalent circuit for the composite network is shown in Figure 4. Two modes with distinct eigenmode impedances are decoupled during each stage by selecting appropriate values for the elements of the stage network. In [10], circuit elements (X_1, B_1), (X_2, B_2) and (X_3, B_3) were obtained by setting $Z_c' = Z_e'$, $Z_b'' = Z_c''$ and $Z_a''' = Z_b'''$,
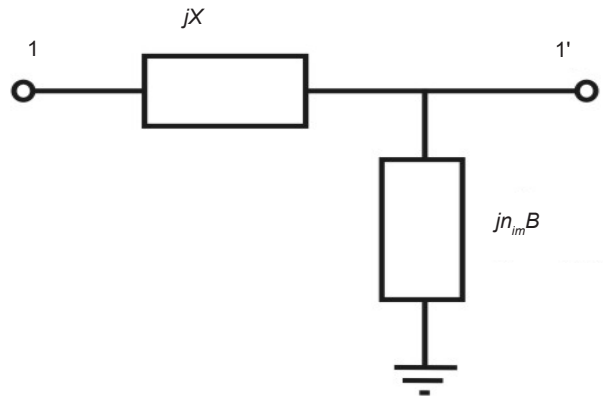
Table 1: Stage networks for equalizing modal impedances of a 6-element array

Network type i	Stage network	Parameter n_{im} in Figure 1
1		$n_{1a} = 0$
		$n_{1b} = 4$
		$n_{1c} = n_{1d} = 3$
		$n_{1e} = n_{1f} = 1$
2		$n_{2a} = n_{2b} = 0$
		$n_{2c} = n_{2d} = n_{2e} = n_{2f} = 3$
3		$n_{3a} = 0$
		$n_{3b} = n_{3c} = n_{3d} = n_{3e} = n_{3f} = 1$

Figure 1: Equivalent circuit of the stage network i when mode m is excited.
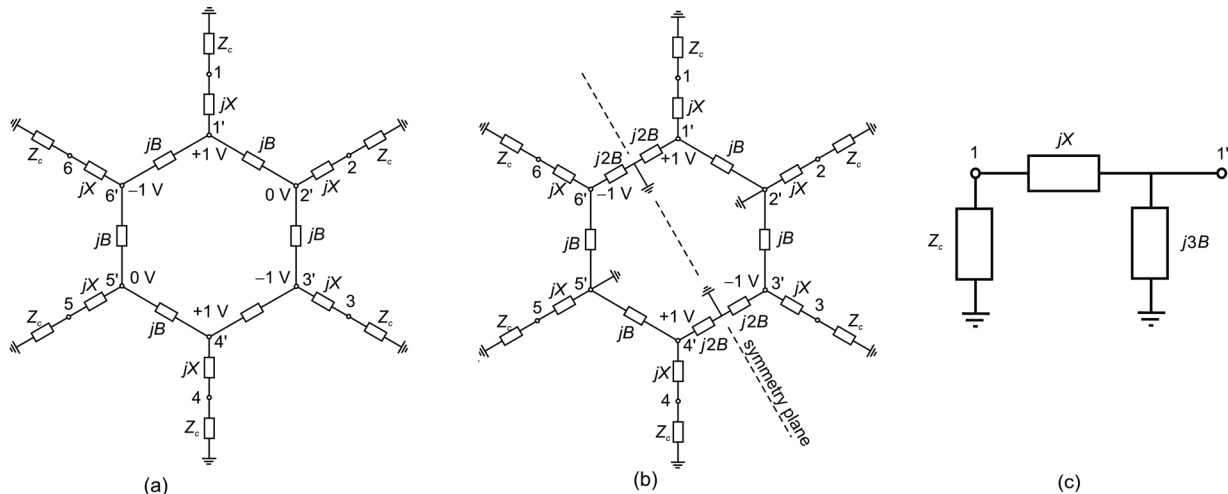

(a)

(b)

(c)

Figure 2: Derivation of equivalent circuit of the stage network 1 when mode c is excited.

and using closed-form expressions to determine the component values. Note that an implementation of the composite decoupling network shown in Figure 3 would require a multilayer circuit board or air bridge crossover structures.

In the alternative approach, we replace the Type 2 network with another Type 1 network in the composite decoupling network. The resulting composite network and its equivalent circuit are shown in Figures 5 and 6, respectively. From Figure 6, the input impedance observed at Ports 1' and 1" for mode m are given by
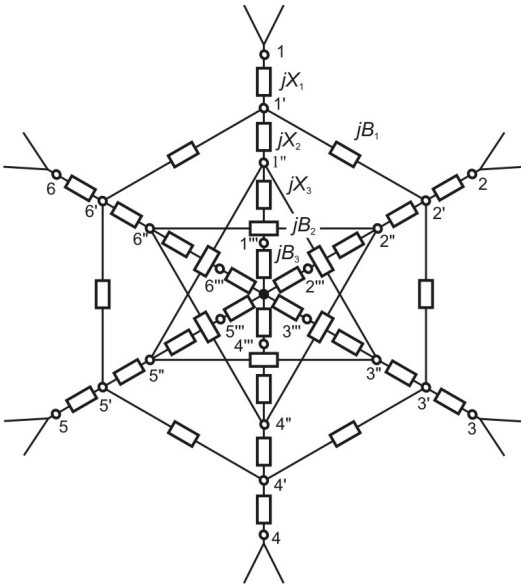
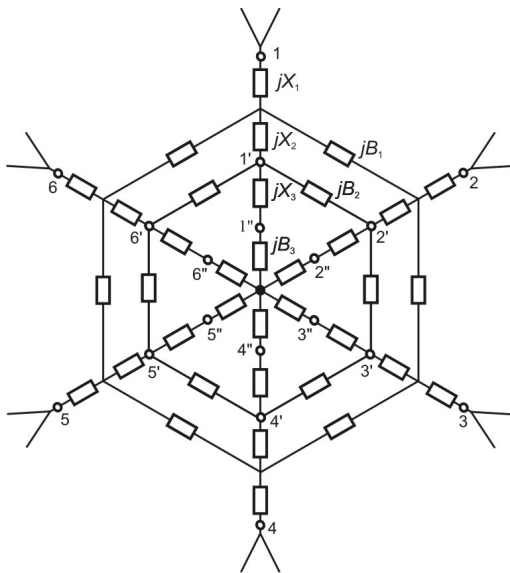**Figure 3:** Composite decoupling network for a 6-element circulant symmetric array [10].

Figure 5: New composite decoupling network for a 6-element circulant symmetric array.

$$Z'_m = \left(\left(\left((Z_m + jX_1)^{-1} + jn_{1m}B_1 \right)^{-1} + jX_2 \right)^{-1} + jn_{1m}B_2 \right)^{-1} \quad (7)$$

and

$$Z''_m = \left((Z'_m + jX_3)^{-1} + jn_{3m}B_3 \right)^{-1}. \quad (8)$$

In this case, network elements (X_1, B_1, X_2, B_2) are obtained by numerically solving the following set of nonlinear equations:

$$\text{Re}[Z'_b - Z'_c] = 0, \quad \text{Im}[Z'_b - Z'_c] = 0$$
$$\text{Re}[Z'_b - Z'_e] = 0, \quad \text{Im}[Z'_b - Z'_e] = 0. \quad (9)$$

The remaining network elements are found in closed form as $X_3 = g(Z''_a, Z''_b)$ and $B_3 = h(Z''_a, n_{3a}, Z''_b, n_{3b}, X_3)$, where the functions g and h are defined in [10]. This network is suitable for single-layer circuit board implementation.

To verify the theory, a decoupling network for a 6-element monopole array was designed and analyzed. As in [10], the six elements of the array are evenly distributed on a circle with radius of 15 mm (0.125λ at a center frequency of f_0 = 2.5 GHz). Each monopole has a length of 28 mm (0.23λ) and a diameter of 1 mm (0.0083λ). With a system impedance of Z_0=50Ω, the array's S-parameters were computed at f_0 using CST Microwave Studio [11]. Four distinct sets of solutions for the values of the elements of the decoupling network in Figure 5 can be found. The S-parameters of the array and one set of solutions are shown in Table 2. The elements of an L-section impedance matching networks are also shown, with B_4 being the susceptance of a parallel element to ground and X_4 the reactance of a series element. The scattering parameters
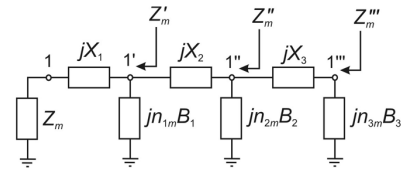

Figure 4: Equivalent circuit of the composite decoupling network in Figure 3 when mode m is excited. The values of n_{1m}, n_{2m} and n_{3m} are specified in Table 1.
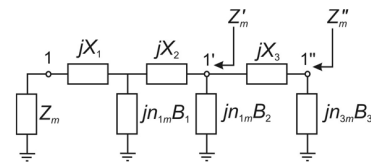

Figure 6: Equivalent circuit of new composite decoupling network in Figure 5 when mode m is excited. The values of n_{1m} and n_{3m} are specified in Table 1.

were computed over a frequency range of $0.98 f_0$–$1.02 f_0$. The results are shown in Figure 7. The array is decoupled and matched at the design frequency f_0, thus illustrating the validity of the theory. The array will be decoupled at f_0 for each of the four solution sets for the elements of the decoupling network, although the scattering parameters of the four networks are not identical. Each network will excite the array elements in a unique way, but internal coupling (via the decoupling network) and external mutual coupling will effectively cancel each other at f_0. Figure 8 shows the radiation patterns of the coupled array and decoupled arrays (both single-layer and multilayer) when only a single port is excited. For the coupled array, the other elements are parasitic radiators excited through mutual coupling alone. On the other hand, all array elements of the decoupled arrays are driven when a single external port is excited. The radiation patterns for the coupled and decoupled arrays in Figure 8 therefore differ markedly. The radiation pattern of the array with the single-layer decoupling network also differs from the one for multilayer network due to variations in the element excitations.

2.2 Design Example: 8-Element Array

The impedance matrix of an 8-element circulant symmetric array is given by

$$
\mathbf{Z^a} =
\begin{bmatrix}
Z_{11}^a & Z_{12}^a & Z_{13}^a & Z_{14}^a & Z_{15}^a & Z_{14}^a & Z_{13}^a & Z_{12}^a \\
Z_{12}^a & Z_{11}^a & Z_{12}^a & Z_{13}^a & Z_{14}^a & Z_{15}^a & Z_{14}^a & Z_{13}^a \\
Z_{13}^a & Z_{12}^a & Z_{11}^a & Z_{12}^a & Z_{13}^a & Z_{14}^a & Z_{15}^a & Z_{14}^a \\
Z_{14}^a & Z_{13}^a & Z_{12}^a & Z_{11}^a & Z_{12}^a & Z_{13}^a & Z_{14}^a & Z_{15}^a \\
Z_{15}^a & Z_{14}^a & Z_{13}^a & Z_{12}^a & Z_{11}^a & Z_{12}^a & Z_{13}^a & Z_{14}^a \\
Z_{14}^a & Z_{15}^a & Z_{14}^a & Z_{13}^a & Z_{12}^a & Z_{11}^a & Z_{12}^a & Z_{13}^a \\
Z_{13}^a & Z_{14}^a & Z_{15}^a & Z_{14}^a & Z_{13}^a & Z_{12}^a & Z_{11}^a & Z_{12}^a \\
Z_{12}^a & Z_{13}^a & Z_{14}^a & Z_{15}^a & Z_{14}^a & Z_{13}^a & Z_{12}^a & Z_{11}^a
\end{bmatrix}. \tag{10}
$$

The eigenvalues of $\mathbf{Z^a}$ are
$Z_a = Z_{11}^a + 2Z_{12}^a + 2Z_{13}^a + 2Z_{14}^a + Z_{15}^a$,
$Z_b = Z_{11}^a - 2Z_{12}^a + 2Z_{13}^a - 2Z_{14}^a + Z_{15}^a$,
$Z_c = Z_d = Z_{11}^a - 2Z_{13}^a + Z_{15}^a$,
$Z_e = Z_f = Z_{11}^a - \sqrt{2}Z_{12}^a + \sqrt{2}Z_{14}^a - Z_{15}^a$, and
$Z_g = Z_h = Z_{11}^a + \sqrt{2}Z_{12}^a - \sqrt{2}Z_{14}^a - Z_{15}^a$,
while the corresponding orthogonal eigenvectors are
$\mathbf{e}_a = [1, 1, 1, 1, 1, 1, 1, 1]^T$, $\mathbf{e}_b = [1, -1, 1, -1, 1, -1, 1, -1]^T$, $\mathbf{e}_c = [1, 1, -1, -1, 1, 1, -1, -1]^T$, $\mathbf{e}_d = [1, -1, -1, 1, 1, -1, -1, 1]^T$, $\mathbf{e}_e = [\sqrt{2}, -1, 0, 1, -\sqrt{2}, 1, 0, -1]^T$, $\mathbf{e}_f = [1, -\sqrt{2}, -1, 0, -1, \sqrt{2}, -1, 0]^T$, $\mathbf{e}_g = [\sqrt{2}, 1, 0, -1, -\sqrt{2}, -1, 0, 1]^T$ and $\mathbf{e}_h = [1, \sqrt{2}, 1, 0, -1, -\sqrt{2}, -1, 0]^T$. The four stage networks that can be used to decouple the eigenmodes of this array are shown in Table 3. Each stage network will again reduce to the

Table 2: Scattering parameters and decoupling network elements for the 6-element array

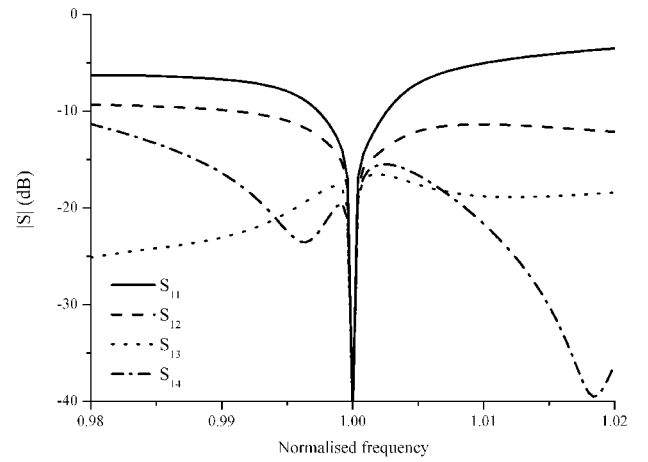| Array scattering parameters	$S_{11}^a = -6.79$ dB $\angle 159.3°$
	$S_{12}^a = -7.96$ dB $\angle 4.5°$
	$S_{13}^a = -15.33$ dB $\angle -53.4°$
	$S_{14}^a = -17.93$ dB $\angle -101.5°$
Decoupling network elements	$X_1 = 6.3077$, $B_1 = 0.0827$
	$X_2 = 9.0252$, $B_2 = 0.2770$
	$X_3 = -5.7862$, $B_3 = -0.1203$
Decoupled port impedance (Ω)	$Z_{11}''' = 142.68 - j64.63$
Matching network elements	$B_4 = 0.0064$, $X_4 = 78.0858$

Figure 7: Scattering parameters of the decoupled and matched 6-element array versus normalized frequency, f/f_0.
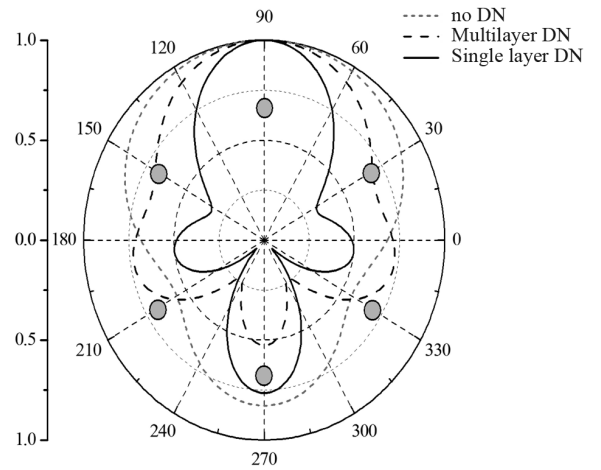

Figure 8: Normalized radiation pattern of the 6-element array with and without the decoupling network. The pattern is obtained by feeding port 1 and terminating the other ports in matched loads. Excitation at subsequent ports will cause the radiation pattern to be rotated by 60°.

equivalent circuit shown in Figure 1 when an eigenmode is excited, with parameter n_{im} defined in Table 3. Instead of using a composite decoupling network which consists of a tandem connection of the four stage networks, we follow the alternative approach by employing three Type 1 circuits and one Type 4 circuit to obtain the composite network shown in Figure 9. The equivalent circuit of the composite decoupling network in Figure 10 can be used to calculate the impedance observed at Ports 1' and 1" for mode m as

$$Z'_m = \left(\left(\left(\left(\left((Z_m + jX_1)^{-1} + jn_{1m}B_1 \right)^{-1} + jX_2 \right)^{-1} + jn_{1m}B_2 \right)^{-1} \right.\right.$$
$$\left.\left. + jX_3 \right)^{-1} + jn_{1m}B_3 \right)^{-1} \tag{11}$$

and

$$Z''_m = \left((Z'_m + jX_4)^{-1} + jn_{4m}B_4 \right)^{-1} . \tag{12}$$

The network elements $(X_1, B_1, X_2, B_2, X_3, B_3)$ are obtained by solving the following set of nonlinear equations:
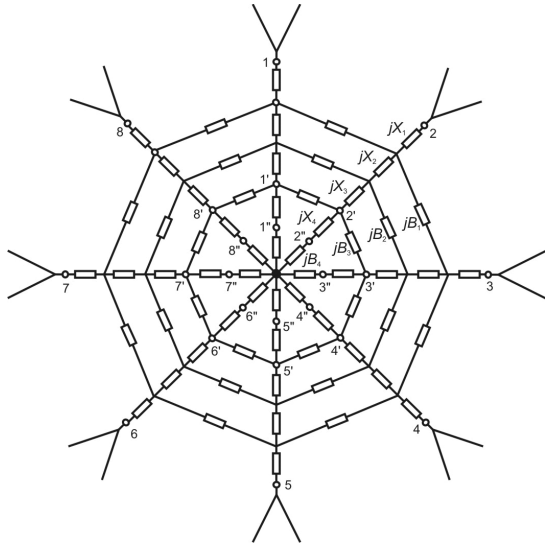
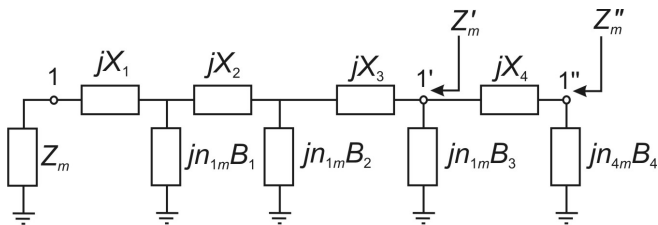**Figure 9:** Composite decoupling network for an 8-element circulant symmetric array.

Figure 10: Equivalent circuit of composite decoupling network in Figure 9 when mode m is excited. The values of n_{1m} and n_{4m} are specified in Table 3.

$$\mathrm{Re}[Z'_b - Z'_c] = 0, \quad \mathrm{Im}[Z'_b - Z'_c] = 0$$
$$\mathrm{Re}[Z'_b - Z'_e] = 0, \quad \mathrm{Im}[Z'_b - Z'_e] = 0$$
$$\mathrm{Re}[Z'_b - Z'_g] = 0, \quad \mathrm{Im}[Z'_b - Z'_g] = 0. \tag{13}$$

The remaining network elements are found in closed form as $X_4 = g(Z''_a, Z''_b)$ and $B_4 = h(Z''_a, n_{4a}, Z''_b, n_{4b}, X_4)$, where the functions g and h are defined in [10].

A decoupling network was designed for an 8-element monopole array with elements evenly distributed on a circle with radius of 15 mm (0.125λ at a center frequency of $f_0 = 2.5$ GHz). Each monopole has a length of 28 mm (0.23λ) and a diameter of 1 mm (0.0083λ). The computed scattering parameters of the array are shown in Table 4. One of the several sets of solutions for the values of the elements of the decoupling network is also shown in Table 4, together with the elements of an L-section impedance matching network, B_5 and X_5. The computed scattering parameters over a frequency range of $0.98 f_0 - 1.02 f_0$ are plotted in Figure 11, while Figure

Table 3: Stage networks for equalizing modal impedances of an 8-element array

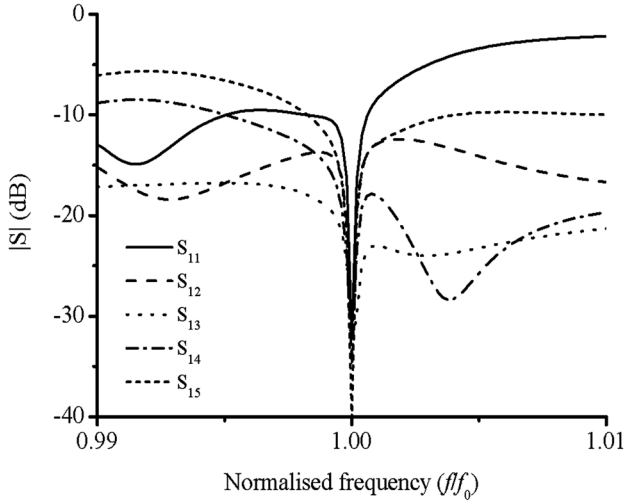| Network type i	Stage network	Parameter n_{im} in Figure 1
1		$n_{1a} = 0$ $n_{1b} = 4$ $n_{1c} = n_{1d} = 2$ $n_{1e} = n_{1f} = 2 + \sqrt{2}$ $n_{1g} = n_{1h} = 2 - \sqrt{2}$
2		$n_{2a} = n_{2b} = 0$ $n_{2c} = n_{2d} = 4$ $n_{2e} = n_{2f} = n_{2g} = n_{2h} = 2$
3		$n_{3a} = n_{3b} = n_{3c} = n_{3d} = 0$ $n_{3e} = n_{3f} = n_{3g} = n_{3h} = 1$
4		$n_{4a} = 0$ $n_{4b} = n_{4c} = n_{4d} = n_{4e}$ $= n_{4f} = n_{4g} = n_{4h} = 1$

Figure 11: Scattering parameters of the decoupled and matched 8-element array versus normalized frequency.

Table 4: Scattering parameters and decoupling network elements for the 8-element array

Array scattering parameters	$S_{11}^a = -5.92$ dB $\angle 167.6°$
	$S_{12}^a = -7.73$ dB $\angle 13.8°$
	$S_{13}^a = -13.42$ dB $\angle -27.9°$
	$S_{14}^a = -19.95$ dB $\angle -85.0°$
Decoupling network elements	$X_1 = 1.803$, $B_1 = 0.1810$
	$X_2 = 0.9561$, $B_2 = -0.8834$
	$X_3 = 0.6937$, $B_3 = 0.2840$
	$X_4 = 2.1582$, $B_4 = 0.1191$
Matching network elements	$B_5 = 0.00573$, $X_5 = 97.4250$

12 shows the radiation pattern of the array when port 1 is excited.

3.   Conclusion

We successfully illustrated an alternative design of DN for circulant symmetric arrays. The procedure is theoretically applicable to arrays of various sizes. Although the design is more complex in that it requires the numerical solution of simultaneous nonlinear equations, it holds a distinct advantage in terms of the ease of implementation. The decoupling network can be implemented on a single layer without any air bridge crossover structures.

References

1.   J. H. Winters, J. Salz, and R. D. Gitlin. "The impact of antenna diversity on the capacity of wireless communication systems",
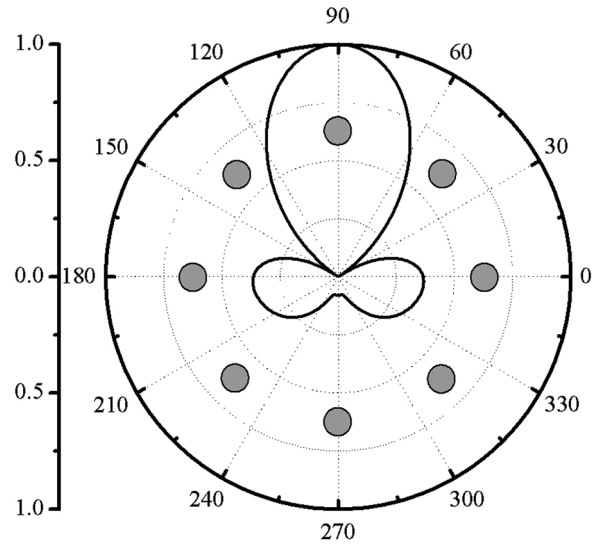

Figure 12: Normalized radiation pattern of the decoupled 8-element array obtained by feeding port 1 and terminating the other ports in matched loads. Excitation at subsequent ports will cause the radiation pattern to be rotated by 45°.

IEEE Trans. Communications, vol. 42, pp. 1740-51, Feb./ Mar./ Apr. 1994.

2.   I. J. Gupta, and A. A. Ksienski. "Effect of mutual coupling on the performance of adaptive arrays", IEEE Trans. Antennas Propagat., vol. 31, no. 5, pp. 785-91, Sep. 1983.

3.   H. J. Chaloupka, and X. Wang. "Novel approach for diversity and MIMO antennas at small mobile platforms", in Proc. IEEE Int. Symp. on Personal, Indoor and Mobile Radio Communications, Barcelona, pp. 637- 42, Sep. 2004,.

4.   J. B. Anderson, and H. H. Rasmussen. "Decoupling and descattering networks for antennas", IEEE Trans. Antennas Propag., vol. 24, no. 6, pp. 841-6, Nov. 1976.

5.   H. J. Chaloupka, X. Wang, and J. C. Coetzee. "Performance enhancement of smart antennas with reduced element spacing", in Proc. IEEE Conf. Wireless Communications and Networking, New Orleans, pp. 425-30, Mar. 2003.

6.   H. J. Chaloupka, X. Wang, and J. C. Coetzee. "Superdirective 3-element array for adaptive beamforming", Microw. Opt. Technol. Lett., vol. 36, no. 6, pp. 425-30, Mar. 2003.

7.   P. T. Chua, and J. C. Coetzee. "Microstrip decoupling networks for low-order multi-port arrays with reduced element spacing", Microw. Opt. Technol. Lett., vol. 46, no. 6, pp. 592-7, Sep. 2005.

8.   H. J. Chaloupka, Y.-H. Lu, and J. C. Coetzee. "A dual-polarized microstrip antenna array with port decoupling for MIMO systems", in Proc. International Symposium on Antennas and Propagation, Sendai, Japan, pp. 1229-32, Aug. 2004.

9.   S.-C. Chen, Y.-S. Wang, and S.-J. Chung. "A decoupling technique for increasing the port isolation between two strongly coupled antennas", IEEE Trans. Antennas Propagat., vol. 56, pp. 3650-8, Dec. 2008.

10.   J. C. Coetzee, and Y. Yu. "Design of decoupling networks for circulant symmetric antenna arrays", IEEE Antennas Wireless Propagat. Lett., vol. 8, pp. 291-4, 2009.

11.   CST Studio Suite 2010, Computer Simulation Technology AG, Darmstadt, Germany.

AUTHORS

Jacob Coetzee was born in South Africa in 1964. He received the B.E. and M.E. Degrees (both with distinction) in 1986 and 1989 and a Ph.D. in electronic engineering from the University of Pretoria in 1994. He was with the Department of Electrical and Electronic Engineering, University of Pretoria from 1994 to 1997 and the Department of Electrical and Computer Engineering, National University of Singapore from 1998 to 2007. He joined the School of Engineering Systems, Queensland University of Technology, Australia in 2008, where he is a Senior Lecturer. His research interests include antenna design, antenna arrays and passive microwave components.

E-mail: jacob.coetzee@qut.edu.au

James D. Cordwell was born in Queensland, Australia in 1987. He graduated from Queensland University of Technology in 2009, with a Bachelor of Mathematics and Electrical Engineering. He currently works as a software engineer for the company GBST which develop software for the financial services industry. His research interests include passive microwave components and antennae array design.

Elizabeth Underwood was born in Queensland, Australia in 1986. She graduated from Queensland University of Technology in 2010 with a B. Mathematics (Distinction) and a B. Electrical & Computer Engineering (Hons). She is currently a full-time mother of two children. Her research interests includes antenna array design and MIMO wireless channel modelling.

Shauna Waite was born in Brisbane in 1988. She recieved a Bachelor of Mathematics (with Distinction) and Electrical Engineering (Hons) both in 2009. She is currently working as an electrical engineer in the building services and infrastructure industry. Her research interests include antenna arrays, control systems and passive microwave components.